Fermi National Accelerator Laboratory

FERMILAB-Conf-96/402-E

CDF

Quarkonia Production at CDF

V. Papadimitriou
For the CDF Collaboration
Physics Department, Texas Tech University
Box 41051, Lubbock, Texas 79409-1051

Fermi National Accelerator Laboratory
P.O. Box 500, Batavia, Illinois 60510

November 1996

Published Proceedings of *Quarkonium Physics Workshop*, University of Illinois at Chicago, Chicago, Illinois, June 1996.

Disclaimer

Distribution

International Journal of Modern Physics A,

CDF/PUB/BOTTOM/PUBLIC/3722
FERMILAB-CONF-96/402-E

QUARKONIA PRODUCTION AT CDF

VAIA PAPADIMITRIOU
Physics Department, Texas Tech University , Box 41051
*Lubbock, TX 79409-1051, U.S.A**

In this paper we present results on J/ψ, $\psi(2S)$, χ_c and Υ production at $\sqrt{s} = 1.8$ TeV. These results were obtained from data taken with the CDF detector at Fermilab. We cover recently completed analyses of the 1992-95 collider run. We find an excess of J/ψ, $\psi(2S)$ and Υ production compared with the predictions from the Color Singlet Model. Prospects for the near future are also discussed.

1. Introduction

The study of quarkonia has yielded valuable insight into the nature of strong interactions since the discovery of the J/ψ in 1974. As far as the strong interactions are concerned, heavy quarkonia are the next simplest particles after leptons and electroweak gauge bosons. In addition, the charmonium and bottomonium systems exhibit a rich spectrum of orbital and angular excitations and therefore they can potentially provide more information than leptons and electroweak gauge bosons. Quarkonia also provide a window in the boundary region between perturbative and non-perturbative QCD and they play a fundamental role in B physics studies. Their production has been recently the subject of a renewed experimental and theoretical interest. The reason is that recent high energy hadron collider experiments have measured the production cross sections for several $Q\bar{Q}$ states and they have been able to disentagle various production mechanisms in the $c\bar{c}$ system providing stringent tests of the production models. The data-theory comparison revealed dramatic discrepancies with production models[1-3] available up to a couple of years ago. These discrepancies have driven theorists to a better understanding of the underlying dynamics and to a more solid theoretical framework within which to operate. The data presented here have been collected with the CDF[4,5] detector during the 1992-1995 Collider Run at Fermilab. This paper is organised as follows. In section 2 we describe results on charmonia physics, in section 3 we present results on Υ production and in section 4 we present conclusions and discuss the future prospects.

*Assistant Professor, vaia@fnald.fnal.gov

Published Proceedings Quarkonium Physics Workshop, University of Illinois at Chicago, Chicago, IL, June 1996

2. Charmonia Production

In this section we describe studies on the production of J/ψ's, $\psi(2S)$'s and χ_c's. In $p\bar{p}$ collisions, J/ψ's and $\psi(2S)$'s come from direct production or from the decay of b hadrons. J/ψ's can be additionally produced through radiative decays of χ_c mesons. Finally, the χ_c mesons are produced directly or from the decay of b hadrons.

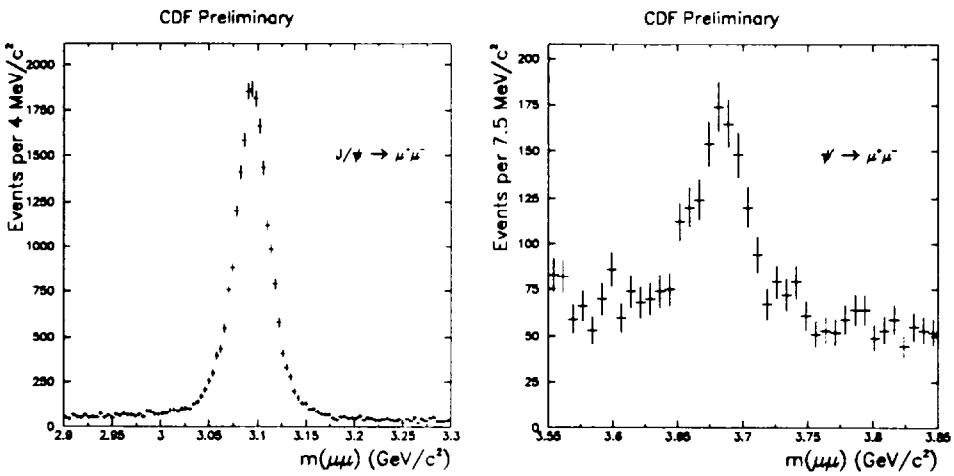

Fig. 1. Invariant mass distribution of the dimuon pair for J/ψ (left) and $\psi(2S)$(right) candidates after all selection requirements.

Using 15.4(17.8) pb^{-1} of data we measured the differential and integrated production cross sections for $J/\psi(\psi(2S))$. The two charmonium states are reconstructed in the dimuon channel and, to remain in the region of good trigger efficiency, one muon is required to have $P_T > 2.8$ GeV/c, while the other muon is required to have $P_T > 2.0$ GeV/c. The J/ψ and $\psi(2S)$ states are reconstructed in the kinematic range $P_T > 5$ GeV/c and $|\eta| < 0.6$ and the mesurements are based on 22,120±161 J/ψ's and 808±46 $\psi(2S)$'s (see Fig.1). The integrated cross sections in the above kinematic range were found to be $\sigma(p\bar{p} \to J/\psi X) \cdot Br(J/\psi \to \mu^+\mu^-) = 17.4 \pm 0.1(\mathbf{stat})^{+2.6}_{-2.8}(\mathbf{sys})$ nb and $\sigma(p\bar{p} \to \psi(2S)X) \cdot Br(\psi(2S) \to \mu^+\mu^-) = 0.57 \pm 0.04(\mathbf{stat})^{+0.08}_{-0.09}(\mathbf{sys})$ nb. Using information from the Silicon Vertex Detector (SVX) to reconstruct the decay vertices of the charmonium states, we distinguish between charmonia from b decays and from other production mechanisms. The SVX detector covers the luminous region of $|z| < 26$ cm along the beam line and only about 50-60% of the tracks found by the Central Tracking Chamber have SVX confirmation. Therefore, in order to decrease the statistical errors on the measurement of the fractions of charmonia coming from b decays, an additional data sample of ~90 pb^{-1} was used for those studies. This data sample is not included in the cross section measurement because the trigger and reconstruction efficiencies are

still under study. Fig. 2 shows the fractions of J/ψ and $\psi(2S)$ from b decays as a function of P_T. We find that for the kinematic region $P_T > 5$ GeV/c and $|\eta| < 0.6$, (19.2±0.2(stat)±0.4(sys))% of J/ψ's and (23.3±1.8(stat)±0.5(sys))% of $\psi(2S)$'s come from the decay of b hadrons. In Fig. 3 (left) the differential production cross section measurements for J/ψ and ψ(2S) from b hadron decays are compared with the theoretical predictions. These cross sections are extracted by convoluting the differential b fraction with the differential J/ψ and $\psi(2S)$ inclusive cross sections. The theoretical predictions were calculated by generating b quarks according to the NLO QCD predictions[6] using a scale $\mu = \mu_0 \equiv \sqrt{m_b^2 + P_T^2}$ and $m_b = 4.75$ GeV/c^2. The b quarks were fragmented into b-flavored hadrons using the Peterson fragmentation[7] with the Peterson fragmentation parameter, ϵ_b, set to 0.006. The B mesons were decayed to a J/ψ or a $\psi(2S)$ with a parametrization of the momentum distribution measured by the CLEO experiment[8]. The uncertainty in the theoretical cross section (shown as the dashed curve) is estimated by setting the scale μ to $\mu_0/4$, ϵ_b to 0.004 and $m_b = 4.5$ GeV/c^2. We see that the experimental measurements are a factor of 3-4 above the central value of the theoretical predictions.

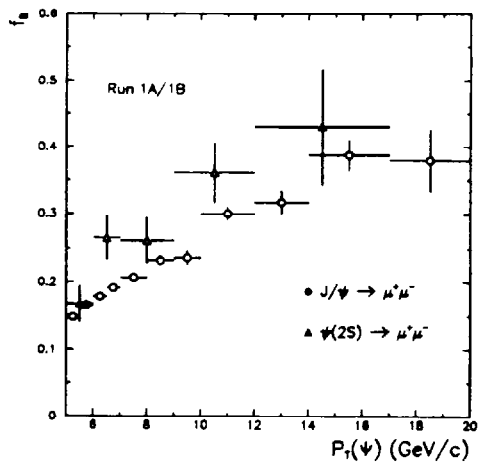

Fig. 2. Fraction of J/ψ and $\psi(2S)$ originating from b hadron decays as a function of P_T.

During the past couple of years it was established that the observed CDF yield for prompt (not originating from b decays) J/ψ's and $\psi(2S)$'s[9,10] is much larger than the theoretical expectation from direct production models including contributions from charm fragmentation and gluon fragmentation from color-singlet diagrams[11,12]. As is evident from Fig. 3 (right), both the J/ψ and $\psi(2S)$ cross sections are higher than theoretical predictions based on the Color Singlet Model (CSM) by a factor of ~ 6 for J/ψ's and a factor ~ 50 for $\psi(2S)$'s. This discrepancy

has created intense theoretical interest[13-19] and it suggests that there are other important mechanisms for direct production of $^3S_1$ states at large P_T beyond those that have already been calculated in CSM. As a result additional theoretical work was completed and for the first time the color-octet fragmentation diagrams were considered as a possible solution for the J/ψ and $\psi(2S)$ anomalies [16-19]. CDF was able to test these theoretical assumptions for both the J/ψ and $\psi(2S)$ states. This became possible, especially for the J/ψ, after the measurement of the fraction of J/ψ's from χ_c decays.

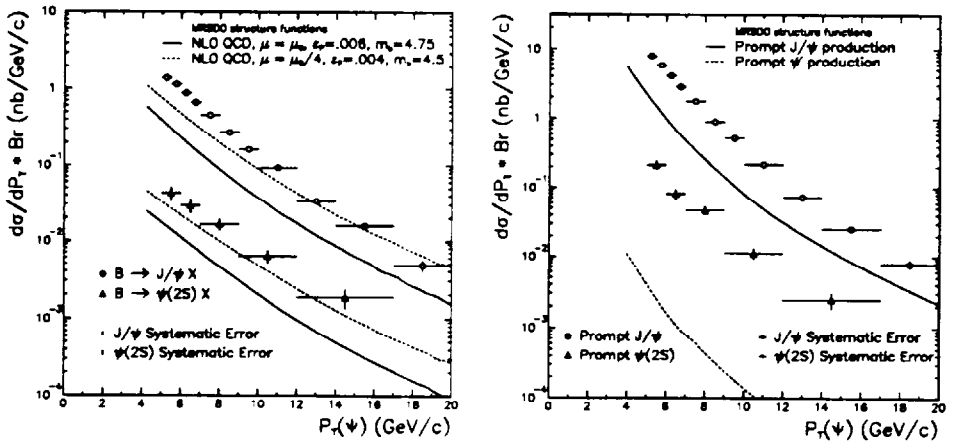

Fig. 3. On the left, differential cross sections from b production of J/ψ and of $\psi(2S)$ as a function of P_T, compared with NLO QCD theoretical expectations; On the right, prompt differential cross sections of J/ψ and of $\psi(2S)$ as a function of P_T compared with the theoretical expectations based on the Color Singlet Model.

We measure the fraction of J/ψ's from χ_c decays by reconstructing the decay chain $\chi_c \rightarrow J/\psi\gamma$; $J/\psi \rightarrow \mu^+\mu^-$ in ~ 18 pb^{-1} of data. We select photon candidates by demanding an electromagnetic energy deposition with at least 1 GeV at the calorimeter and a cluster in the electromagnetic strip chambers. We also require that no tracks point to the calorimeter tower corresponding to the photon candidate. The J/ψ is combined with photon candidates to form the invariant mass difference distribution, $\Delta M = M(\mu^+\mu^-\gamma) - M(\mu^+\mu^-)$, which is shown in Fig. 4 (left). A clear χ_c signal of $1,230 \pm 72$ events is present near $\Delta M = 400$ MeV/c^2 but the individual χ_{c1} and χ_{c2} states are not resolved. The mass resolution predicted by the detector simulation is 50 and 55 MeV/c^2 for the χ_{c1} and χ_{c2} respectively and is not good enough to observe the individual states separated by 45.6 MeV/c^2.

We find that the fraction of inclusive J/ψ's coming from χ_c's, integrated for $P_T^{J/\psi} > 4$ GeV/c and $|\eta^{J/\psi}| < 0.6$, is $F_\chi^{J/\psi} = 28.8 \pm 1.7(stat) \pm 6.4(syst)\%$. This fraction includes a contribution from $B \rightarrow \chi_c X$ decays in the numerator and from $B \rightarrow J/\psi X$ decays in the denominator. The fraction of J/ψ's from χ_c's not

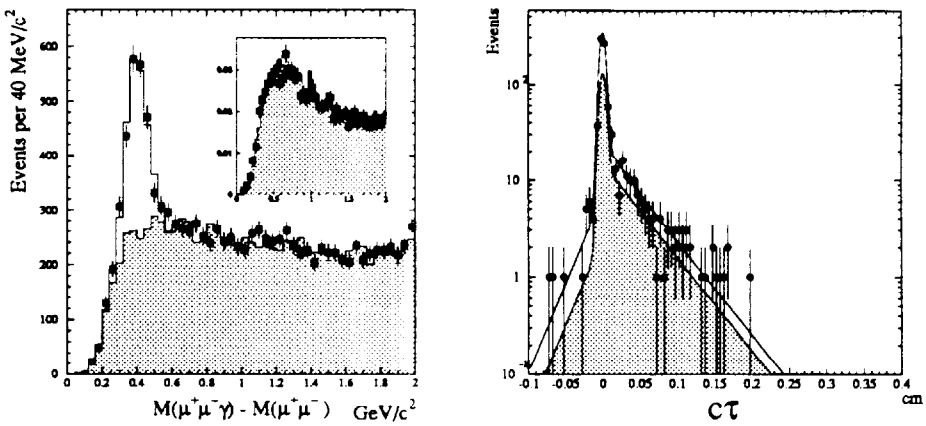

Fig. 4. On the left, the mass difference $M(\mu^+\mu^-\gamma) - M(\mu^+\mu^-)$ for the J/ψ signal region. The points represent the data. The shaded histogram is the background shape predicted by our background Monte Carlo. The solid line is the fit to the data of a gaussian signal plus the background histogram. The inset shows the comparison between data and background Monte Carlo for dimuon in the J/ψ sidebands. On the right, the $c\tau$ distribution for $J/\psi\gamma$ combinations in the χ_c signal region and J/ψ fully reconstructed in the SVX. The points represent the data. The shaded area shows the contribution from the background.

including contributions from b decays is calculated according to the equation:

$$F(No\ b)_{\chi}^{J/\psi} = F_{\chi}^{J/\psi} \cdot \frac{1 - F_b^{\chi}}{1 - F_b^{J/\psi}} \tag{1}$$

where F_b^{χ} is the fraction of reconstructed χ_c's from b decays and $F_b^{J/\psi}$ is the fraction of reconstructed J/ψ's from b decays. The fraction F_b^{χ} was extracted by fitting the $c\tau$ distribution of $J/\psi\gamma$ combinations in the χ_c signal region to the sum of two functions, one associated with the χ_c signal and one associated with its background (see Fig. 4 (right)). The J/ψ's are fully reconstracted in the SVX and each function is the sum of a zero lifetime component and a long lived component where the lifetime of the long lived component is fixed to the average b lifetime of 438 μm measured by CDF[20]. The result of the fit is $F_b^{\chi} = (10.8 \pm 3.1)\%$. Using $F_b^{J/\psi}$ $= (17.8 \pm 0.2\ (\mathrm{stat}) \pm 0.4(\mathrm{sys}))\%$ in the kinematic region $P_T^{J/\psi} > 4$ GeV/c and $|\eta^{J/\psi}| < 0.6$, the correction factor is $(1\text{-}F_b^{\chi})/(1\text{-}F_b^{J/\psi}) = 1.085 \pm 0.04$. A Monte Carlo simulation shows that this correction factor is constant as a function of $P_T^{J/\psi}$ and therefore we use this correction factor for all P_T bins. The resulting fraction of J/ψ's from χ_c's, for $P_T^{J/\psi} > 4$ GeV/c and $|\eta^{J/\psi}| < 0.6$, not including contributions from b hadron decays is $F(Nob)_{\chi}^{J/\psi} = 31.2 \pm 1.8(stat) \pm 7.1(syst)\%$. Fig. 5 shows this fraction as a function of $P_T^{J/\psi}$. This implies that the production from χ_c's is not the dominant production mechanism of prompt J/ψ's, in disagreement

with current theoretical predictions not including color-octet diagrams for the J/ψ production. The differential cross section of prompt J/ψ's from χ_c decays in Fig. 6 (left) was obtained by parametrising the fraction $F(Nob)_\chi^{J/\psi}$ as a function of $P_T^{J/\psi}$ with an exponential function and convoluting it with the differential prompt J/ψ cross section. The direct J/ψ cross section, that is prompt J/ψ's not from χ_c's, was obtained by subtraction. The curves are the color-singlet theoretical calculation based on references[11,12]. The calculation for direct J/ψ production is a factor of $\sim$ 50 below the experimental cross section. This indicates that CSM underestimates direct production of the J/ψ by the same factor found for the $\psi(2S)$ and that direct production is the dominant source of prompt J/ψ's.

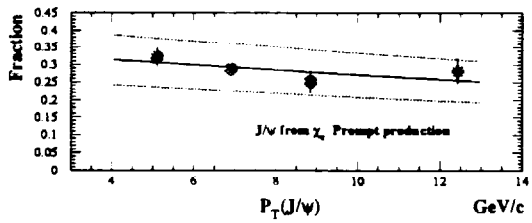

Fig. 5. The fraction of J/ψ from χ_c as a function of $P_T^{J/\psi}$ with the contribution from b's removed. The error bars shown represent the statistical uncertainty. The solid line corresponds to an exponential parametrization of the fraction. The dashed lines correspond to a $\pm$ 23% systematic uncertainty.

At CDF we reconstruct alternatively the χ_c signal through the detection of conversion photons. In $\sim$ 110 pb^{-1} of data, we see 93.8 ± 11.8 χ_{c1}'s and 51.0 ± 9.8 χ_{c2}'s (see Fig. 6 (right)). Prompt χ_{c1}'s and χ_{c2}'s are isolated by imposing the requirement that the proper lifetime, λ, of the $J/\psi - \gamma$ system is less than 100 μm. It was found that for prompt events $\frac{\sigma(\chi_{c2})}{\sigma(\chi_{c1})+\sigma(\chi_{c2})} = 0.47 \pm 0.08(\text{stat}) \pm 0.02(\text{syst.})$

The direct, differential J/ψ and $\psi(2S)$ cross sections are shown in Fig 7. The open circles represent the data. The b and χ_c components have been removed from the J/ψ cross section and the b component has been removed from the $\psi(2S)$ cross section. The theory curves are from Ref.[19]. The dashed curves represent the prediction from CSM. The $\psi(2S)$ feeddown curve in the J/ψ cross section plot is a properly normalised contribution from the decay $\psi' \rightarrow J/\psi\pi^+\pi^-$. The dotted curves correspond to the production in the $^3S_1$ color-octet state and the dashed-dotted curves to the production in the $^3P_0$ and $^1S_0$ color-octet states. The shapes of these color-octet cross sections are calculated perturbatively. The normalisation nevertheless depends on non-perturbative matrix elements, for which there exist only order of magnitude predictions, and therefore the matrix elements are derived from fits to the CDF data. We fit simultaneously the J/ψ and $\psi(2S)$ curves. In this fit all the correlations between the J/ψ and the $\psi(2S)$ are taken into account. Since the theory predicts that the $^3S_1^{(8)}$ and the $^1S_0^{(8)}, ^3P_0^{(8)}$ amplitudes should be

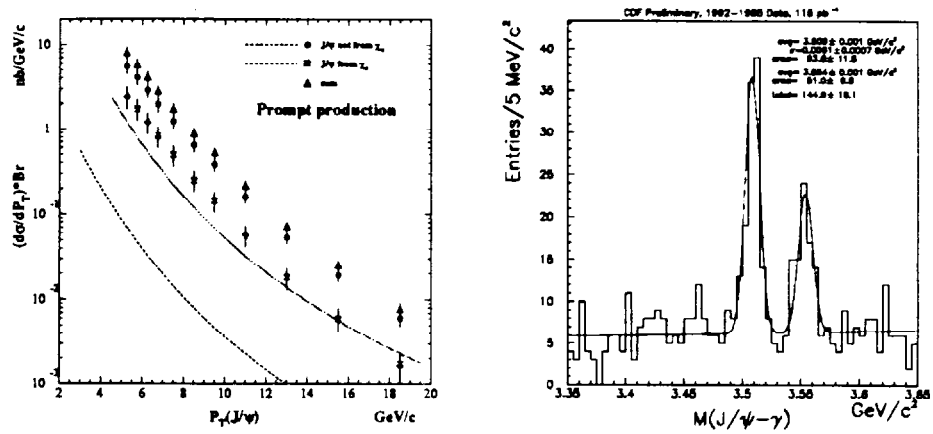

Fig. 6. On the left, the differential cross sections of prompt J/ψ as a function of $P_T^{J/\psi}$ with the contribution from b's removed. The dashed curve is the Color Singlet calculation for J/ψ production. The solid curve is the calculation for $\chi_c \rightarrow J/\psi\gamma$ production and includes both Color Singlet and Color Octet contributions. On the right, The mass difference $M(\mu^+\mu^-\gamma) - M(\mu^+\mu^-)$ for the J/ψ signal region and for $P_T^\gamma > 1\ GeV/c$, where tracking information is used for the detection of the photon. The events are promptly produced.

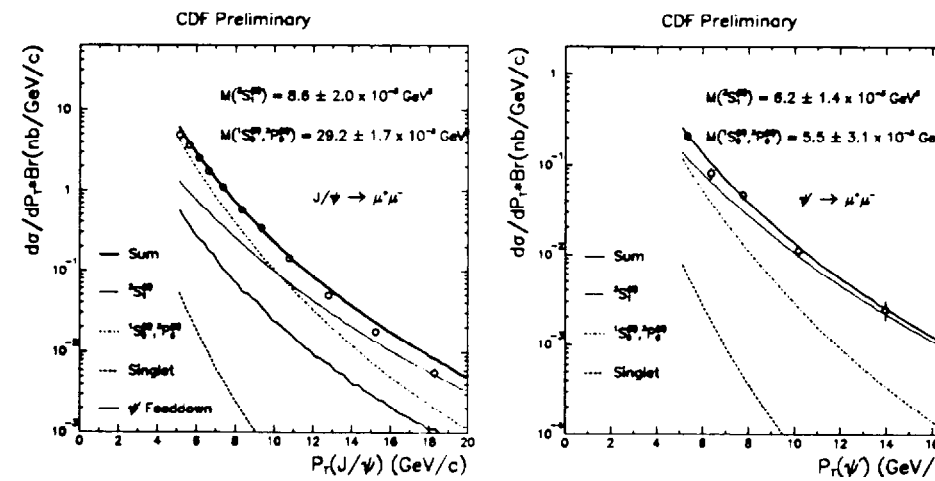

Fig. 7. Differential cross sections of J/ψ as a function of $P_T^{J/\psi}$ (left) and of $\psi(2S)$ as a function of $P_T^{\psi(2S)}$ (right). The b contribution has been removed from both J/ψ and $\psi(2S)$ and the χ_c contribution has been removed from J/ψ. The ratio of the ${}^3S_1^{(8)}$ and ${}^1S_0^{(8)}, {}^3P_0^{(8)}$ amplitudes has been required to be the same for J/ψ and $\psi(2S)$.

similar for the J/ψ and $\psi(2S)$, we impose the additional constraint that the ratio of the two amplitudes be the same for J/ψ and for $\psi(2S)$. Although the fit is above the J/ψ data at high P_T, the overall agreement with the data is good.

3. Υ Production

It is expected that the Υ's resonances are produced directly or from the decay of higher mass χ_b states. The CDF experiment studies Υ production by studying the reaction $p\bar{p} \rightarrow \Upsilon X \rightarrow \mu^+\mu^- X$. Since, as discussed above, the measurements of prompt J/ψ and $\psi(2S)$ production cross sections are higher than the theoretical predictions, it is of interest to carry out similar comparisons for the Υ particles.

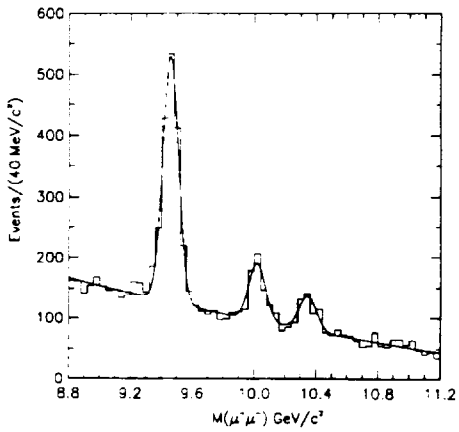

Fig. 8. The CDF invariant mass distribution for $\Upsilon(1S)$, $\Upsilon(2S)$ and $\Upsilon(3S)$.

We measured[21] the differential and integrated production cross sections of the Υ(1S), Υ(2S) and Υ(3S) states using a data sample of 16.6 pb^{-1}. In the kinematic region $|y| < 0.4$ and P_T >0.0 GeV/c, 1,274 Υ(1S), 320 Υ(2S) and 196 Υ(3S) events were reconstructed (see Fig. 8). The differential cross section measurements for the Υ(1S), Υ(2S) and Υ(3S) states are shown in Fig. 9 along with the color-singlet theoretical calculation[19].

The integrated cross section results divided by the rapidity bin width are:

$$d\sigma/dy(\bar{p}p \rightarrow \Upsilon(1S), y = 0, 0 < P_t < 16\ \mathrm{GeV/c}) \times Br = 753 \pm 29\ (\mathrm{stat}) \pm 72\ (\mathrm{sys})\ \mathrm{pb}$$
$$d\sigma/dy(\bar{p}p \rightarrow \Upsilon(2S), y = 0, 1 < P_t < 10\ \mathrm{GeV/c}) \times Br = 183 \pm 18\ (\mathrm{stat}) \pm 24\ (\mathrm{sys})\ \mathrm{pb}$$
$$d\sigma/dy(\bar{p}p \rightarrow \Upsilon(3S), y = 0, 1 < P_t < 10\ \mathrm{GeV/c}) \times Br = 101 \pm 15\ (\mathrm{stat}) \pm 13\ (\mathrm{sys})\ \mathrm{pb}$$

where Br stands for the branching ratio of the corresponding Υ state to $\mu^+\mu^-$. The ratios of the integrated cross section results were also computed in the range

$1 < P_t < 10$ GeV/c and for $|y| < 0.4$. The results are $\sigma Br(\Upsilon(2S))/\sigma Br(\Upsilon(1S)) = 0.281 \pm 0.030(\text{stat}) \pm 0.038(\text{sys})$ and $\sigma Br(\Upsilon(3S))/\sigma Br(\Upsilon(1S)) = 0.155 \pm 0.024(\text{stat}) \pm 0.021(\text{sys})$. The rate of Υ production for all three states was found to be higher than color-singlet QCD calculations. Inclusion of color-octet production mechanisms seem to help explain some of the discrepancies[19].

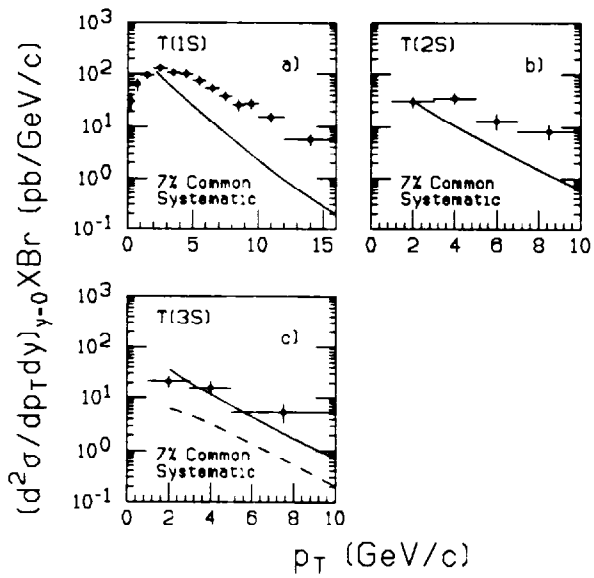

Fig. 9. The product $(d^2\sigma/dP_t dy)_{y=0} \times Br$ vs. P_t for $\Upsilon(1S) \rightarrow \mu^+\mu^-$, $\Upsilon(2S) \rightarrow \mu^+\mu^-$, $\Upsilon(3S) \rightarrow \mu^+\mu^-$, where Br stands for the branching ratio of the corresponding Υ state to $\mu^+\mu^-$ and y stands for the rapidity of the Υ state. The Color Singlet calculation from Ref.[19], is also shown. (a) The theoretical prediction includes contributions from direct $\Upsilon(1S)$ production and $\chi_b(1P)$ and $\chi_b(2P)$ decay. (b) The theoretical prediction includes contributions from direct $\Upsilon(2S)$ production and $\chi_b(2P)$ decay. (c) The dashed line corresponds to the direct $\Upsilon(3S)$ production contribution and the solid line corresponds to the sum of the contributions from the direct $\Upsilon(3S)$ production and the decay of the unobserved $\chi_b(3P)$ state.

4. Conclusions-Prospects

In conclusion CDF has studied charmonium and bottomonium production and has made measurements which are in disagreement with conventional theoretical expectations. The color-octet mechanism seems to help explain some of the discrepancies[19]. Much more experimental and theoretical work is necessary though in order to show conclusively that heavy quarkonia production mechanisms are understood.

Currently, in 110 pb^{-1} of data, we have a sample of $\sim$ 500,000 J/ψ's in the rapidity region ($|\eta| < 1$), from which $\sim$ 244,000 are reconstructed at the SVX. We have also large samples of $\psi(2S)$'s in both the $\mu^+\mu^-$ and $J/\psi\pi^+\pi^-$ modes, χ_c's and

Υ's. The completion of the analysis of these data sets from the 1992-1995 Collider Run will shed, we hope, more light on the quarkonia production mechanisms. The increase of statistics will be particularly useful for the measurement of the spectra of the $\psi(2S)$, χ_{c1}, χ_{c2}, Υ(2S) and Υ(3S) states and for the rapidity dependence of the quarkonia cross sections. The measurement of the spin alignment of the J/ψ, $\psi(2S)$, χ_{c1} and χ_{c2} and the three Υ states will also produce very valuable information on the production mechanisms. The increase of statistics, combined with refinement in technique should also allow us to measure the production cross section of χ_b states and thus understand better the bottomonia production mechanisms.

Acknowledgements

We thank the Fermilab staff and the technical staffs of the participating institutions for their vital contributions. This work was supported by the U.S. Department of Energy and National Science Foundation; the Italian Istituto Nazionale di Fisica Nucleare; the Ministry of Education, Science and Culture of Japan; the Natural Sciences and Engineering Research Council of Canada; the National Science Council of the Republic of China; and the A. P. Sloan Foundation.

References

1. R. Baier and R. Rückl, *Z. Phys. C19*, (1983) 251.
2. E.W.N. Glover, A.D. Martin, W.J. Stirling, *Z. Phys. C38*, (1988) 473.
3. G.A. Schuler, CERN-TH.7170 (1994).
4. F. Abe *et al.*, *Nucl. Instr. Meth. A271*, (1988) 387.
5. D. Amidei *et al.*, *Nucl. Instr. Meth. Phys. Res., Sect. A350*, (1994), 73.
6. P. Nason, S. Dawson and R.K. Ellis, *Nucl. Phys. 327*, (1988) 49.
7. C. Peterson *et al.*, *Phys. Rev. D27*, (1983) 105.
8. R. Balest *et al.*, "Inclusive Decays of B mesons to Charmonium", CLNS 94/1315.
9. The CDF Collaboration, "Study of Production Mechanisms of J/ψ and ψ(2S)", FERMILAB-CONF-94/136-E.
10. The CDF Collaboration, "J/ψ and ψ(2S) Production at CDF", FERMILAB-CONF-96/156-E.
11. E. Braaten, M. Doncheski, S. Fleming, M. Mangano, *Phys. Lett. B333*, (1994) 548.
12. M. Cacciari, M. Greco, *Phys. Rev. Lett. 73*, (1994) 1586.
13. E. Close, *Phys. Lett. B342* (1995) 369.
14. P. Cho, S. Trivedi, M. Wise, *Phys. Rev. D51*, (1995) 2039.
15. D.P. Roy, K. Sridhar, *Phys. Lett. B345*, (1995) 537.
16. E. Braaten and S. Fleming, *Phys. Rev. Lett. 74*, (1995) 3327.
17. P. Cho and M. Wise, *Phys. Lett. 346*, (1995) 129.
18. M. Cacciari, M. Greco, M.L. Mangano, A. Petrelli, *Phys. Lett. 356*, (1995) 553.
19. P. Cho and A.K. Leibovich, *Phys. Lett. D53*, (1996) 150,
    P. Cho and A.K. Leibovich, *Phys. Rev. D53*, (1996) 6203.
20. F. Abe *et al.*, *Phys. Rev. Lett. 71*, (1993) 3421.
21. F. Abe *et al.*, *Phys. Rev. Lett. 75*, (1995) 4358.